ELSEVIER

Journal of Nuclear Materials 266–269 (1999) 217–221

journal of nuclear materials

Section 2. Contributed oral papers

Molybdenum erosion measurements in Alcator C-Mod

W.R. Wampler [a,*], B. LaBombard [c], B. Lipschultz [c], G.M. McCracken [b], D.A. Pappas [c], C.S. Pitcher [c]

[a] *Sandia National Laboratories, Department 1111, MS 1056, P.O. Box 5800, Albuquerque, NM 87185-1056, USA*
[b] *JET Joint Undertaking, Abingdon Oxon, OX14 3EA, UK*
[c] *Plasma Science and Fusion Center, Massachusetts Institute of Technology, Cambridge, MA 02139, USA*

Abstract

Erosion of molybdenum was measured on a set of 21 tiles after a run campaign of 1090 shots in the Alcator C-Mod tokamak. The net erosion of molybdenum was determined from changes in the depth of a thin chromium marker layer measured by Rutherford backscattering. Net Mo erosion was found to be approximately 150 nm near the outer divertor strikepoint and much less everywhere else. Gross erosion rates by sputtering were estimated using ion energies and fluxes obtained from Langmuir probe measurements of edge-plasma conditions. Predicted net erosion using calculated gross erosion with prompt redeposition agrees with measured net erosion within a factor of three. Sputtering by impurities, mainly boron, dominates erosion.

Keywords: Alcator C-Mod; Erosion; Molybdenum; Ion-beam analysis

1. Introduction

Erosion of plasma-facing surfaces is one of the most serious issues facing long-pulse fusion devices. However, net erosion is the combined result of complex processes including sputtering by deuterium and by heavier plasma impurities, transport of eroded material by the plasma and redeposition. Measurements of net erosion by tokamak plasmas are therefore needed to predict long term erosion. Net erosion rates exceeding 3 nm/s or 10 cm/exposure-year have been measured on graphite divertor plates in DIII-D [1]. This erosion rate would be unacceptably high in a long pulse fusion reactor. One way to reduce the erosion rate is through the use of high-Z materials, which are expected to erode more slowly than low-Z materials because of their lower sputtering yields. Here we examine erosion of molybdenum in Alcator C-Mod, in which all plasma-contacting surfaces are Mo tiles. The net Mo erosion, after a run campaign of 1090 shots was determined from changes in the depth of a thin chromium marker layer measured by Rutherford backscattering. Gross erosion by sputtering was estimated using ion energies and fluxes obtained from Langmuir probe measurements of edge-plasma conditions. Comparison between measured net erosion and predicted gross erosion indicates that sputtering by plasma impurities, mainly boron, must dominate Mo erosion.

2. Experimental method

In these experiments, a subsurface layer of chromium was used as a depth marker to measure net erosion of Mo from the surface of tiles. The depth of the Cr layer beneath the surface was measured by Rutherford backscattering before and after the tiles were exposed to tokamak plasmas. A set of 21 tiles were prepared with the buried Cr marker layer. The tiles were first metallographically polished to prepare a smooth surface. Thin films of chromium and then molybdenum were evaporated onto the tiles over a circular region 13 mm in diameter at the center of each tile. Before plasma exposure, RBS spectra were taken on each tile using 2.5 MeV ^{4}He, from which it was determined that the

* Corresponding author. +1 505 844 4114; fax: +1 505 844 7775; e-mail: wrwampl@sandia.gov.

0022-3115/99/$ – see front matter
PII: S0022-3115(98)00663-1

thickness of the Cr layer was 100 nm and the thickness of the Mo overlayer ranged from 300 to 600 nm.

The tiles were installed in the Alcator C-Mod tokamak and exposed to 1090 tokamak plasmas during the period from November 1995 to March 1996. The location of the tiles during the exposure is shown in Fig. 1. Plasma conditions during the exposure were typically, $n_e = (1–5) \times 10^{20}$ m^{-3}, $I_p = 0.6–1.2$ MA, $B_T =$ 3–8 T, plasma duration 1 s, plasma heating power up to 5 MW, power flux densities on the divertor plates up to 10 MW m^{-2}. The total integrated time of exposure to tokamak plasmas was about 1200 s.

After exposure, the tiles were removed from the tokamak and again examined by ion-beam analysis. Fig. 2 shows RBS spectra taken using 2.5 MeV ^{4}He on tile 18 from the outer strikepoint (OSP) and tile 3 from the inner wall. Fig. 2(a) illustrates how the thickness of the Mo overlayer was determined from the RBS spectra. After scattering from Mo at the external surface, He ions have an energy of about 2.1 MeV due to the kinematics of elastic scattering. He ions scattered from Mo beneath the surface reach the detector with lower energy due to the continuous energy loss of ions as they pass through material on the way in, before scattering and back out after scattering. The dip in the spectra is due to the Cr marker layer. The flat-topped feature of the spectra between the dip and the surface edge is due to scattering from Mo in the overlayer. Since the stopping power of energetic ions in materials is known [2], the width of this feature gives the thickness of the Mo overlayer [3]. The decrease in width of this feature (indicated by the arrow) corresponds to a reduction in Mo overlayer thickness from 340 to 220 nm for this tile.

Many of the tiles had a layer of low-Z material on the surface. This layer was examined by RBS using 2.5 MeV ^{4}He and 1.7 MeV ^{1}H and by nuclear reaction analysis (NRA) using the ^{11}B(p,α)^{8}Be reaction with an analysis beam of 650 keV protons. These studies showed the low-Z surface layer to consist mainly of boron. In addition to boron, this low-Z surface layer could contain small amounts (few percent) of other low-Z elements such as carbon and oxygen. The thickness of this boron layer was determined by RBS. The step in yield in the RBS

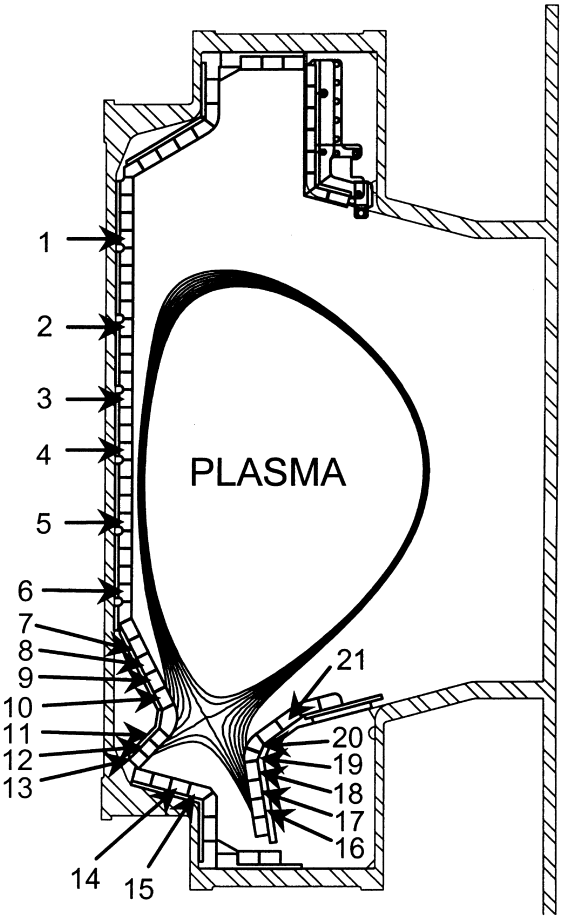

Fig. 1. Diagram of Alcator C-Mod showing the location of the 21 tiles with the Cr depth marker.

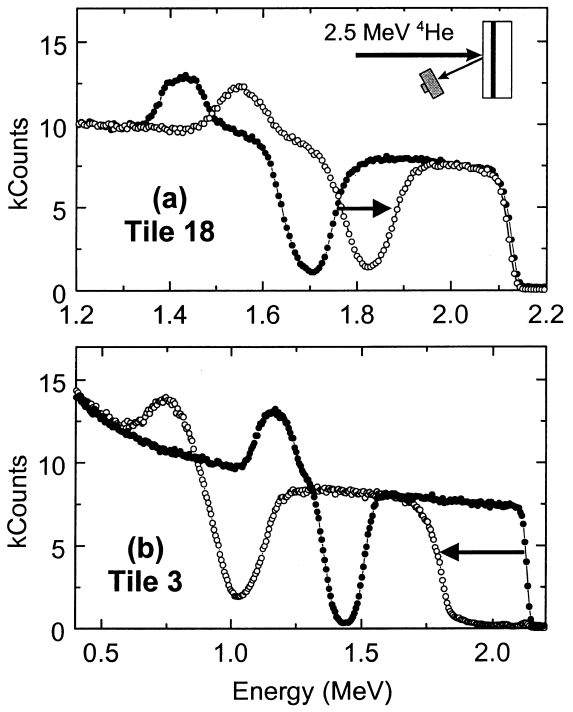

Fig. 2. RBS spectra taken with 2.5 MeV ^{4}He before (filled circles) and after (open circles) exposure to C-mod plasmas. Tile 18 from the OSP shows the effect of a reduction in Mo overlayer thickness from 340 to 220 nm with very little boron deposition. Tile 3 from the inner wall shows little change in Mo overlayer thickness but a shift down in energy by ~0.34 MeV due to deposition of about 0.5 μm of boron on the surface.

spectrum due to scattering from Mo at the surface is shifted down in energy because of energy loss by the ions as they pass through the boron layer, as indicated by the arrow in Fig. 2(b). Using the known stopping power of ions in boron [2], the thickness of the boron layer is obtained from the magnitude of this energy shift. The boron is present because the vessel was boronized several times during the run campaign. Boron was deposited by decomposition of diborane in a plasma to reduce plasma impurities.

NRA was also used to measure deuterium (D) on the tiles. This measurement used the ^{3}He(d,p)α nuclear reaction with an analysis beam of 700 keV ^{3}He. The areal density of D within about 1 μm of the surface was determined from the yield of energetic protons.

3. Experimental results

The results from ion-beam analysis of the tiles are summarized in Fig. 3. The net Mo erosion was highest on tiles 17–20 at the OSP. Here the erosion was 100–170 nm. The Mo erosion was much less on all other tiles including the inner strikepoint (ISP). The thickness of the boron surface layer is also shown in Fig. 3. The OSP had the least boron. Boron coverage was also relatively low at the ISP. Elsewhere, boron coverages were higher, ranging up to 1.8×10^{19} atoms/cm^2, which corresponds to a physical thickness of 1.4 μm assuming the density 2.34 g/cm^3 of elemental boron. On some of the tiles (tile numbers 4,5,7,8,9,10,14,15,21) the boron layer was found to have nonuniform thickness over the region of the analysis beam spot (1×1 mm). This caused a broadening of the edges in the RBS spectra used to determine the thickness of both the boron and Mo layers and a corresponding reduction in the precision of the value obtained for the thickness of these layers. The larger error bars on the boron thickness and Mo erosion shown in Fig. 3 for these tiles are due to this effect.

Fig. 3 shows the deuterium coverage on the tiles. The error bars for these data indicate the range of values measured at several locations on each tile. The OSP had the least D which is consistent with results from Mo erosion and B deposition which indicate that the OSP is a region undergoing net erosion of material.

B and D coverages on the nose tile of the ISP (between tiles 10 and 11 in Fig. 1) were measured and are plotted in Fig. 3 at tile number 10.5. However, this tile did not have the buried Cr depth marker and so the Mo erosion could not be determined for this tile.

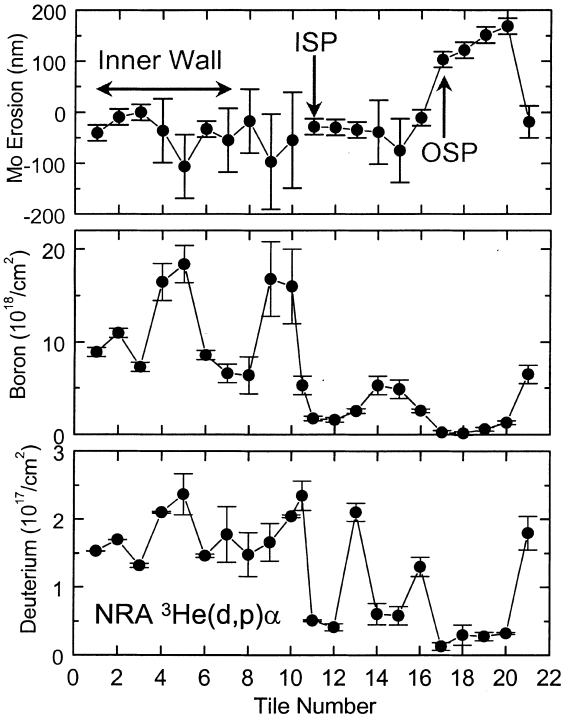

Fig. 3. Results from ion-beam analysis. Measured net Mo erosion (top), thickness of surface boron layer (center) and areal density of deuterium (bottom). At the OSP (tiles 16–20) Mo erosion is highest but boron and D deposition is lowest.

4. Calculated erosion based on physical sputtering

The outer divertor plate is instrumented with built-in Langmuir probes, which are able to deduce the incident plasma particle flux density, local plasma density and electron temperature. These probes were operated routinely throughout the campaign in which the tiles were exposed. From the probe measurements it is possible to make estimates of the gross erosion on the tiles, integrated over the campaign. The results are shown in Fig. 4.

We assume physical sputtering is the dominant erosion mechanism, including sputtering by the background fuel ions D^+, the dominant impurity boron and some amount of molybdenum self-sputtering. In the case of boron, a helium-like B^{3+} charge state is assumed. Normal incidence sputtering yields for D and B are used, since numerical studies indicate only a weak dependence on angle of incidence [4]. This is in contrast to molybdenum, where a relatively strong angular dependence exists at energies near the threshold for sputtering [4]. In this case, we use the sputtering yield at 18° off-normal incidence, as this angle is roughly the average angle of incidence for promptly redeposited molybdenum ions [5]. The incident D and B ion energy is determined using a shifted Maxwellian distribution [6], while we estimate the promptly deposited molybdenum ion energy to be $E_0 \sim 5T_e$.

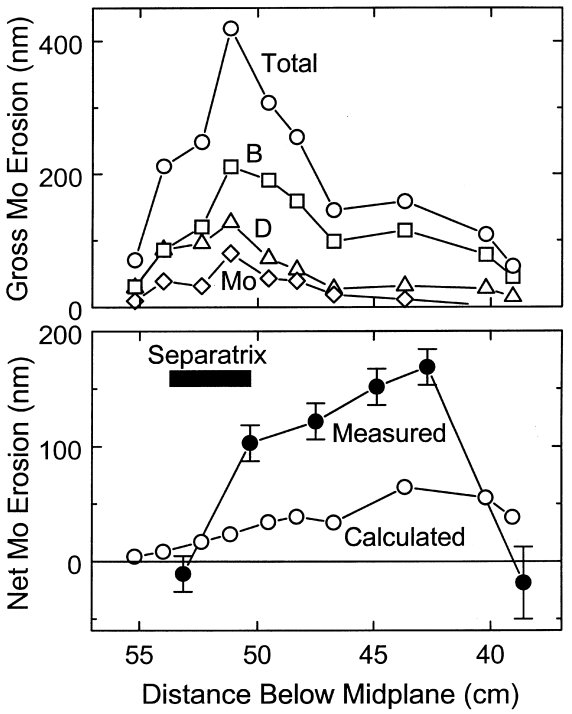

Fig. 4. Gross Mo erosion on the outer divertor (top panel) calculated using Langmuir probe data for D^+, B^{3+}, Mo ions and total, versus distance below the C-Mod midplane. Also shown is the net erosion (bottom panel) calculated using the gross erosion with prompt redeposition (open circles) and measured using the Cr depth marker (filled circles). The typical separatrix position (tiles 17–18) is indicated by the bar, the divertor nose (tile 20) is ~44 cm below the midplane.

The sputtered molybdenum influx density is given by

$$\Phi_{\rm in} = [(j_s/e)\sin(\theta)/(1 + Z_B a)](Y_D + aY_B)/(1 - rY_{Mo}),$$

[7] where j_s is the parallel field ion saturation current density measured by the probes, e the electronic charge, θ the glancing field angle, $Y_{D,B,Mo}$ are the sputtering yields for D^+, B^{3+} and Mo ions, $Z_B = 3$ the boron charge state, a the ratio of boron to deuteron fluxes and r the fraction of sputtered molybdenum atoms which are promptly redeposited. The average charge $Z_{Mo} = +1.5$ is used for the Mo ions [6] for determining Y_{Mo}. The gross erosion as deduced from the Langmuir probe data has been compared at given times throughout the campaign with the intensity of Mo I light emission measured with a multi-chord visible light spectrometer. Since the boron flux ratio is not routinely measured, a has been treated as a fitting parameter to match the observed Mo I influx with the probe calculation of $\Phi_{\rm in}$ [6]. The gross erosion is dominated by impurity sputtering, mainly from boron. The gross sputtering is highly peaked in the vicinity of the separatrix, as expected since this location has on average both elevated incident particle flux, as well as elevated particle energies.

To compare gross erosion estimated from Langmuir probe data with the net erosion measured by the surface marker technique, an estimate of redeposition is required. We have assumed only prompt redeposition, where sputtered Mo atoms, depending on the local plasma conditions, can be ionized at a distance less than one gyro-radius from the plate and thus have a significant chance of being promptly redeposited, i.e.

$$\Phi_{\rm net} = \Phi_{\rm in}(1 - r).$$

Those particles which are not promptly redeposited in this way are assumed to be lost to the plasma, of course ultimately returning to a surface at some point in the vessel, but not strongly influencing the net erosion at the outer plate. We use the simple analytic results from Ref. [8] to determine the prompt redeposition probability. The probe-deduced campaign-integrated gross and net erosion are shown in Fig. 4, along with the marker determined net erosion. In general, good agreement is obtained between the probe result and the marker erosion, both in shape and absolute magnitude.

The shape of the net erosion pattern is markedly different than the gross erosion as shown in Fig. 4. The gross erosion is strongly peaked at the separatrix whereas the net erosion peaks away from the separatrix. This is a result of strong prompt redeposition in the vicinity of the separatrix and relatively weaker redeposition further out in the SOL, i.e. molybdenum sputtered further out in the SOL has a lower probability of being promptly redeposited due to the lower values of plasma density and temperature and hence longer mean-free path for ionization, at this location. This results in a ratio of net to gross erosion of ~0.4 here, compared to ~0.06 near the separatrix. The calculation of erosion from Langmuir probe measurements is described in more detail in Ref. [6].

5. Conclusions

Net Mo erosion after exposure to 1090 plasmas was found to be approximately 150 nm near the outer divertor strikepoint and much less everywhere else. The peak Mo erosion rate averaged over the total 1200 s of exposure is 0.14 nm/s (0.45 cm/exposure-year) which is much lower than erosion rates (>10 cm/exposure-year) for graphite tiles at the OSP in DIII-D [1]. This is qualitatively consistent with the lower erosion for Mo expected from the reduced Mo sputtering yield. Erosion was much less at the ISP than at the OSP. Similar asymmetry between erosion at the ISP and OSP has also been seen on the DIII-D divertor [9]. A surface layer of boron from boronization was found at all locations except near the OSP. It is likely that the Mo was covered by the boron layer for most of the exposure and therefore not directly exposed to plasma except at the OSP

where the boron layer was removed relatively quickly by the plasma.

Gross erosion rates by sputtering were estimated using ion energies and fluxes obtained from Langmuir probe measurements of edge-plasma conditions. Predicted net erosion using calculated gross erosion with prompt redeposition agrees with measured net erosion within a factor of three. Calculated gross erosion is strongly peaked at the separatrix, whereas calculated and measured net erosion are both peaked outside the separatrix. The agreement between measured and calculated net erosion both in magnitude and location, supports the model that the principal mechanism for Mo erosion is physical sputtering by ions, mainly boron.

Acknowledgements

Sandia is a multiprogram laboratory operated by Sandia Corporation, a Lockheed Martin Company, for the US Department of Energy under contract DE-ACO4-94AL85000.

References

[1] D. Whyte et al., J. Nucl. Mater. 241–243 (1997) 660 and this conference.
[2] J.F. Ziegler, The Stopping and Ranges of Ions in Matter, vol. 4, Pergamon Press, New York, 1977.
[3] J.R. Tesmer, M. Nastasi (Eds.), Handbook of Modern Ion Beam Analysis, Materials Research Society, Pittsburgh, 1995.
[4] W. Eckstein, V. Philipps, in: W.O. Hofer, J. Roth (Eds.), Physical Processes of the Interaction of Fusion Plasmas with Solids, Academic Press, New York, 1996.
[5] J.N. Brooks, D.N. Ruzic, J. Nucl. Mater. 176&177 (1990) 278.
[6] D.A. Pappas et al., these Proceedings.
[7] P.C. Stangeby, in: D.E. Post, R. Behrisch (Eds.), Physics of Plasma–Wall Interactions in Controlled Fusion, Plenum, New York, 1986.
[8] D. Naujoks, K. Asmussen, M. Bessenrodt-Weberpals et al., Nucl. Fusion 36 (1996) 671.
[9] C.P.C. Wong, D. Whyte, R.J. Bastasz, J. Brooks, W.P. West, W.R. Wampler, J. Nucl. Mater. 258–263 (1998) 433.